Article

Discovery Medicine 2023; 35(179): 946–955
https://doi.org/10.24976/Discov.Med.202335179.90

β-Sitosterol Enhances Lung Epithelial Cell Permeability by Suppressing the NF-κB Signaling Pathway

Xingdong Chen[1,2,†], Juan Chen[3,†], Yi Ren[4], Mengmeng Wang[1,4], Zhizhou Yang[1,3,4], Wei Zhang[4], Quan Li[3], Chao Liu[4], Zhaorui Sun[1,3,4,*], Shinan Nie[1,3,4,*]

[1]Department of Emergency Medicine, Jinling Hospital, Nanjing School of Clinical Medicine, Southern Medical University, 210002 Nanjing, Jiangsu, China
[2]Department of Critical Care Medicine, Huizhou First Hospital, 516000 Huizhou, Guangdong, China
[3]Nanjing University of Chinese Medicine, 210023 Nanjing, Jiangsu, China
[4]Department of Emergency Medicine, Jinling Hospital, Affiliated Hospital of Medical School, Nanjing University, 210002 Nanjing, Jiangsu, China
*Correspondence: sunzhr84@163.com (Zhaorui Sun); shn_nie@sina.com (Shinan Nie)
[†]These authors contributed equally.
Published: 1 December 2023

Background: The dysregulation between pro-inflammatory and anti-inflammatory responses during sepsis is a crucial factor in driving sepsis progression. Acute lung injury (ALI) resulting from excessive production and accumulation of inflammatory mediators in the lungs contributes to impaired lung barrier function. The activation of the NF-κB signaling pathway during inflammation leads to the transcriptional activation of multiple inflammatory genes. Given the plausible impact of NF-κB signaling suppression in mitigating lung injury, substantive evidence demonstrates beta-sitosterol (BS)'s proficient ability to block NF-κB activation. Therefore, the aim of the present investigation was to delve into the impacts of BS in the context of sepsis-induced acute lung injury, employing both a mouse model and a model involving lung epithelial cells.

Methods: Sepsis-induced lung injury was simulated in mice through cecum ligation and puncture (CLP). To emulate injury in murine lung epithelial (MLE-12) cells, an experiment involving lipopolysaccharide (LPS) was administered. Evaluation of alterations in lung tissue permeability encompassed techniques such as lung wet/dry (W/D) mass ratio, Evans blue staining, and quantification of total protein concentration in bronchoalveolar lavage fluid (BALF). Lung tissue histopathological shifts were ascertained via hematoxylin and eosin (HE) staining. Additionally, the concentrations of inflammatory cytokines IL-6 and TNF-α were quantified in every lung tissue and cell group by implementing enzyme-linked immunosorbent assay (ELISA). Protein quantification for signal biomarkers was carried out using Western blotting and immunofluorescence methodologies. In tandem, the assessment of MLE-12 cell permeability was conducted by evaluating fluorescein isothiocyanate (FITC)-dextran extravasation.

Results: BS mitigated lung tissue pathologies, reduced inflammatory factors, and lowered tissue and cell permeability. BS inhibited NF-κB signaling and increased claudin-4 and claudin-5 expression, enhancing septic lung epithelial cell permeability.

Conclusions: Through suppressing the NF-κB signaling cascade, BS effectively curtails the levels of inflammatory mediators. Simultaneously, it orchestrates the modulation of claudin-4 and claudin-5 expression, culminating in the augmentation of lung epithelial cell barrier competence, thus improving sepsis-induced lung injury.

Keywords: β-sitosterol; sepsis; NF-κB; tight junction; lung injury

Background

Sepsis, a grave medical condition arising from an imbalanced immune reaction triggered by an infection, affects a staggering number of individuals [1], with approximately 48.9 million people affected and resulting in approximately 11 million deaths annually, representing 19.7% of global mortality [2]. The development of sepsis revolves around a disturbance between the counteracting anti-inflammatory and pro-inflammatory reactions [3]. This discordance subsequently triggers the liberation of various inflammatory agents like IL-6, IL-1β, and TNF-α. The influx and accumulation of these agents, coupled with inflammatory cells, within the lung environment can potentially disrupt barrier integrity. This disruption can harm the pulmonary vascular endothelium and alveolar epithelium, progressively resulting in lung injury [4,5]. Lung injury is a common complication in sepsis, impacting approximately 68.2% of patients. It may progress to acute respiratory distress syndrome (ARDS), a condition associated with substantial mortality and presenting significant therapeutic challenges [6].

Claudins are vital transmembrane proteins that form the structural backbone of tight junctions, essential in main-

taining cell permeability [7]. Within respiratory epithelia, Claudin-4 is prominently expressed across various respiratory epithelial cells, reinforcing the alveolar barrier, facilitating alveolar fluid removal, and providing protection during lung injury. Previous observations have shown that enhancing its expression via adenovector expression constructs augments transepithelial resistance by around 30% [8–11]. Similarly, claudin-5 plays a significant role in the paracellular endothelial barrier and in fortifying tight junctions, thereby optimizing the efficacy of the endothelial barrier [12].

Beta-sitosterol (BS), a phytosterol analogous and structurally similar to cholesterol, possesses potent anti-inflammatory properties [13]. It modulates NOD-like receptor protein 3 (NLRP3), an inflammasome located in macrophages, subsequently reducing the production of IL-6, IL-1β, and TNF-α [14]. A study involving septic rats demonstrated BS's ability to mitigate inflammatory responses and inhibit NF-κB activation [15]. Research anterior to this has postulated the involvement of the NF-κB signaling pathway in orchestrating the expression of tight junction proteins—most notably, claudin-4 and claudin-5—known influencers of epithelial barrier function and permeability [16,17]. Drawing inspiration from these insights, we hypothesized that BS might enhance lung tissue impermeability and alleviate sepsis-induced lung injury through NF-κB pathway inhibition and modulation of tight junction proteins. The present study aims to examine this hypothesis and elucidate the potential therapeutic benefits of BS in sepsis-induced lung injury.

Materials and Methods

Animal Model Preparation and Grouping

Male BALB/c mice (8 weeks old; weighing 21–25 g) were sourced from the Model Animal Research Center at Jinling Hospital. They were allowed to acclimate for one week without fasting before the commencement of the experiment. All the procedures and protocols pertaining to the experiments were subjected to thorough review and approval by the Ethics Committee of Jinling Hospital, Nanjing School Clinical Medicine, Southern Medical University (Approval NO. 2022DZGKJDWLS-00160). Subsequently, the mice were allocated randomly into three distinct groups, each consisting of ten mice. Before the surgical procedures, the mice were anesthetized using 26 mg/kg of propofol. The three distinct groups under went a set of procedures tailored to their respective experimental conditions. The initial group underwent a median abdominal incision, revealing the cecum without subsequent ligation or perforation. In place of this, fluid resuscitation involved the administration of 3 mL of physiological saline at intervals of 8 and 16 hours post-sham operation. Designated as the sham-operated control, this group served as the baseline reference. The second cohort encompassed the cecum ligation and puncture (CLP) group, subjected to the ligation and puncture procedure and received 3 mL of saline at matching intervals of 8 and 16 hours post-procedure. Within the third group, labeled as the BS group, intraperitoneal administration of β-sitosterol (1 mg/kg) occurred at the 8th and 16th-hour marks following CLP. To conclude the study, all mice were humanely euthanized by 200 mg/kg sodium pentobarbital injection at the 24th hour [15]. Their lung tissues underwent bronchoalveolar lavage with saline to facilitate subsequent analysis. The obtained bronchoalveolar lavage fluid (BALF) underwent centrifugation at 2000 revolutions per minute (rpm) for 15 minutes using a high-speed refrigerated centrifuge (Heal Force, Shanghai, China) for further testing.

Evans Blue Staining

We employed the Evans Blue tracer method to determine the lung permeability in mice. One hour before euthanasia, mice were intravenously injected with Evans Blue solution (IE0280, Solarbio, Beijing, China). After perfusion with phosphate buffered saline (PBS), the lungs were weighed and immersed in a clean centrifuge tube containing 1 mL of formamide per 100 mg of lung tissue at 37 °C overnight. The absorbance was measured at 620 nm, and a standard curve of Evans Blue concentration was established. Using this standard curve, the amount of Evans Blue leakage (expressed as ug/g of lung tissue) was calculated for each specimen.

BALF Total Protein Detection

The bicinchoninic acid (BCA) protein concentration assay kit (71285-M, Merck, Darmstadt, Germany) was employed to quantify the overall protein content within the BALF, strictly adhering to the instructions provided by the manufacturer.

Lung Wet/Dry (W/D) Weight Ratio

In order to assess pulmonary edema, the wet weight of the left lung in the mice was documented. Following this, the left lung specimens were placed in an oven set at 60 °C for 48 hours to facilitate thorough drying, enabling the subsequent determination of the dry weight. The wet-to-dry weight ratio was computed utilizing the formula W/D = wet weight (g) / dry weight (g).

Histopathological Examination

The lung tissues of mice were fixed using a solution of 10% formaldehyde, then embedded in paraffin and sliced into 4-µm thick sections. These sections underwent staining with hematoxylin and eosin (HE) to visualize potential pathological changes. This staining process was carried out with an optical microscope (Leica DM2500 LED, Wetzlar, Germany). An evaluation system for lung tissue injury was put into action to assess the extent of lung tissue damage quantitatively. This comprehensive scoring system con-

sidered various injury indicators, including alveolar wall edema, hemorrhaging, vascular congestion, and the infiltration of polymorphonuclear leukocytes. The severity of lung injury was categorized into four distinct levels based on the score achieved: scores from 4 to 6 represented mild inflammation, scores from 7 to 9 represented moderate inflammation, and scores from 10 to 12 represented severe inflammation [18].

Cell Culture and Treatment

The murine lung epithelial (MLE-12) cells, which originated from the National Collection of Authenticated Cell Cultures (Shanghai, China, 5301MOU-KCB85024ZJ), underwent rigorous screenings to ensure the absence of mycoplasma infection, yielding negative results. These cells were nurtured within Roswell Park Memorial Institute (RPMI) 1640 medium (Thermo, 8122013, Fisher, Waltham, MA, USA), with supplementation of 10% fetal bovine serum (FBS, F8318, Sigma-Aldrich, St. Louis, MO, USA). Their cultivation was sustained at a temperature of 37 °C within a humidified environment containing 5% CO_2.

To simulate an *in vitro* model of lung injury induced by sepsis, the control group was cultured in the medium until the commencement of experimentation. The lipopolysaccharide (LPS) group was subjected to a 24-hour treatment with 10 µg/mL of LPS (L2630, Sigma-Aldrich). In the LPS + BS group, a 2-hour pre-treatment with 10 µg/mL LPS was followed by a 24-hour incubation with 15 µM BS. Introducing an additional element, the LPS + BS + phorbol 12-myristate 13-acetate (PMA, HY-18739, MedChemExpress, Monmouth Junction, NJ, USA) group underwent a pre-treatment with 15 µM PMA for 1 hour prior to the administration of LPS and BS.

Enzyme-Linked Immunosorbent Assay

TNF-α (PT512, Beyotime, Shanghai, China) and IL-6 (PI326, Beyotime, China) levels were detected in lung tissues and MLE-12 cell supernatants using mouse enzyme-linked immunosorbent assay (ELISA) kits. Perform experiments following the guidelines provided in the operation manual.

Leakage Test of FITC Dextran

To assess the permeability of lung epithelial cells, MLE-12 cells were introduced to the upper chamber of 24-transwell inserts (6.5 mm diameter, 0.4 µm pore size, Labselect, Hefei, China) at a seeding density of $1 \times 10^5/cm^2$. A medium supplemented with 10% serum was positioned in the lower chamber as a chemoattractant to guide the cells' movement. Subsequently, an incubation period of three days ensued, allowing the cells to attain confluence.

For the permeability assessment, 1 mg/mL fluorescein isothiocyanate (FITC)-dextran (HY-128868D, MedChemExpress, Monmouth Junction, NJ, USA) was introduced into the upper chamber. Concurrently, the medium within the lower chamber was replaced. Following an incubation period of one hour, a meticulous extraction of 200 µL from the lower chamber's medium was executed, with subsequent transfer into a 96-well plate boasting a black bottom. The quantification of fluorescence intensity within the samples was achieved using a spectrophotometer equipped with a 488 nm excitation wavelength laser and an emission collection spectrum of 510 nm. By employing the concentration curve as a reference, the concentration of the fluorescent marker in the lower chamber was subsequently ascertained [19].

Western Blotting

Protein samples were obtained from mouse lung tissue and MLE-12 cells by lysing with Radio Immunoprecipitation Assay (RIPA, P0013C, Beyotime, Shanghai, China). Upon quantification through a protein concentration assay kit, the protein samples were separated using sodium dodecyl sulfate-polyacrylamide gel electrophoresis (SDS-PAGE) and subsequently transferred onto membranes composed of polyvinylidene fluoride (PVDF). To initiate the subsequent stages, the PVDF membranes were subjected to a blocking step using 5% skimmed milk. This was followed by an overnight incubation at 4 °C with primary antibodies. After the incubation of primary antibodies (claudin-4, 1:1000, AF5350, Fushen, Shanghai, China; claudin-5, 1:1000, AF0130, Fushen, China; BCL-2, 15071S, 1:1000, Cell Signaling, Danvers, MA, USA; BAX, 41162S, 1:1000, Cell Signaling, USA; NF-κB p65, 1:1000, 8242S, Cell Signaling, USA; Phospho-NF-κB p65, 1:1000, 3033S, Cell Signaling, USA; β-actin, P60709, Abways, Shanghai, China), the membranes were further incubated with a secondary antibody that was conjugated to-horseradish peroxidase (HRP, A0208, Shanghai, Beyotime, China) for 1 hour at room temperature. The ensuing signal was captured using a chemiluminescence image analysis system (Tanon 5200, Tanon Science & Technology Co., Ltd., Shanghai, China) and BeyoECL Moon (P0018FM, Beyotime, Shanghai, China). The protein bands' ensuing grayscale values were analyzed using Image J software (version 1.51, National Institute of Health, Bethesda, MD, USA). The relative expression levels of the target proteins were computed by dividing their respective grayscale values by the grayscale value of β-actin.

Immunofluorescence

Cells were initially seeded at a density of $1 \times 10^5/cm^2$ and allowed to culture within confocal dishes for 24 hours. Upon completing the drug treatment phase, the cells were fixed using a 4% paraformaldehyde solution at room temperature for 10 minutes. Following fixation, a 0.2% Triton-100 solution was introduced to facilitate permeabilization for 5 minutes. Subsequently, goat serum was employed for a 1-hour blocking step. The dilution of either primary or secondary antibodies is 1:200. Primary antibodies were

incubated overnight at 4 °C within a humidified chamber. Moving forward, the cells were introduced to donkey anti-rabbit IgG-Alexa Fluor 594 (2145022, Life Technologies, Carlsbad, CA, USA) for a 45-minute incubation at room temperature, all while carefully shielded from light exposure. A 4′,6-diamidino-2-phenylindole (DAPI) solution (FS1205, Fushen, shanghai, China) was applied for 5 minutes to visualize the cell nuclei. Confocal microscopy (utilizing the Zeiss 800 model, Jena, Germany) was employed for image acquisition. Subsequently, the fluorescence values were subjected to analysis utilizing the Image J software. The relative expression levels of the target proteins were deduced by dividing their respective fluorescence values by the grayscale value of β-actin.

Statistical Analysis

The findings from all conducted experiments were presented in the form of mean values along with their corresponding standard deviations. Statistical evaluation was conducted utilizing the GraphPad Prism 8 software (GraphPad Software, Inc., San Diego, CA, USA). To ascertain potential disparities among the various groups, an initial analysis of variance (ANOVA) was carried out, followed by subsequent application of Tukey's multiple comparisons test. A significance level of $p < 0.05$ was established to determine statistical significance.

Results

BS Increased the Sepsis-Induced Permeability in Lung Tissue and Reduced Sepsis-Induced Lung Injury in Mice

The examination of BALF total protein levels revealed a noteworthy upsurge within the BALF of mice in the CLP group when compared with those in the sham-operated group ($p < 0.01$, Fig. 1A). However, the administration of BS yielded a marked reduction in the total protein content within the BALF of septic mice, showcasing a statistically significant distinction when compared to the CLP group ($p < 0.01$), illustrating diminished inflammatory exudation in the lungs.

Evaluating lung tissue permeability using Evans blue staining (Fig. 1B) revealed that the CLP group had significantly higher permeability levels compared to the sham-operated group ($p < 0.0001$). Remarkably, the introduction of BS highlighted a pronounced improvement in lung tissue conditions in septic mice ($p < 0.001$). The W/D ratio analysis further corroborated these findings (Fig. 1C), with BS treatment leading to reduced W/D ratios in lung tissue ($p < 0.0001$), providing further evidence of its beneficial effects.

Histological evaluations (Fig. 1D) displayed intact structures and typical morphology in the sham-operated group, with no notable inflammatory alterations. Conversely, in the CLP group, inflammatory cells increased in the lung tissues, but BS administration mitigated these adverse effects, reducing inflammation and edema in septic mice.

A marked disparity came to the fore after scrutinizing the lung injury status through the analysis of HE-stained sections (Fig. 1E). Specifically, the mice within the CLP group exhibited considerably elevated lung injury scores, underscoring the severity of the injury compared to the comparatively less affected sham-operated group. In contrast, treatment with BS lowered the lung injury scores of septic mice compared to the CLP group, suggesting alleviation in injury severity ($p < 0.01$).

Mitigation of Inflammation by BS in Septic Mice: Enhanced Claudin-4 and Claudin-5 Expression in Lung Tissue and Suppressed p65 Phosphorylation

A clear contrast emerged between the sham-operated and CLP groups: TNF-α and IL-6 exhibited marked increases within the CLP group, which in turn saw reductions upon subsequent BS treatment ($p < 0.0001$, Fig. 1F,G). Notably, the presence of the anti-apoptotic protein BCL-2 experienced significant diminishment in the CLP group, whereas the proapoptotic protein BAX witnessed elevation. In stark contrast, the application of BS induced a significant surge in BCL-2 and a corresponding drop in BAX, underscoring its preventive influence against apoptosis within septic mice ($p < 0.0001$, Fig. 1H,I).

The examination of claudin-5 and claudin-4 expression levels in lung tissues indicated that the CLP group exhibited considerably lower levels in comparison to the sham-operated group ($p < 0.01$, Fig. 1H,I). However, when subjected to BS treatment, the expression levels of claudin-5 and claudin-4 in lung tissues of septic mice saw a significant upswing. Furthermore, the level of p65 phosphorylation was markedly higher in the CLP group ($p < 0.001$). However, upon BS treatment, there was a conspicuous reduction in p65 phosphorylation, indicating a discernible mitigation of inflammation ($p < 0.05$).

BS Ameliorates Inflammation and Enhances Cell Permeability in LPS-Treated MLE-12 Cells

The results revealed a notable upsurge in the concentrations of TNF-α and IL-6 among MLE-12 cells under inflammatory conditions, namely those stimulated by LPS ($p < 0.0001$, Fig. 2A,B). Notably, the introduction of BS as a treatment agent brought about a noteworthy reduction in the levels of these inflammatory markers ($p < 0.0001$). Furthermore, the application of BS + PMA (p65 agonist) yielded a contrasting result, inducing a substantial escalation in the expression levels of IL-6 and TNF-α ($p < 0.001$, Fig. 3A,B).

The outcomes of the FITC-dextran permeation assay underscored a noteworthy transformation, with the permeability of MLE-12 cells undergoing a substantial elevation subsequent to the influence of LPS stimulation ($p < 0.0001$,

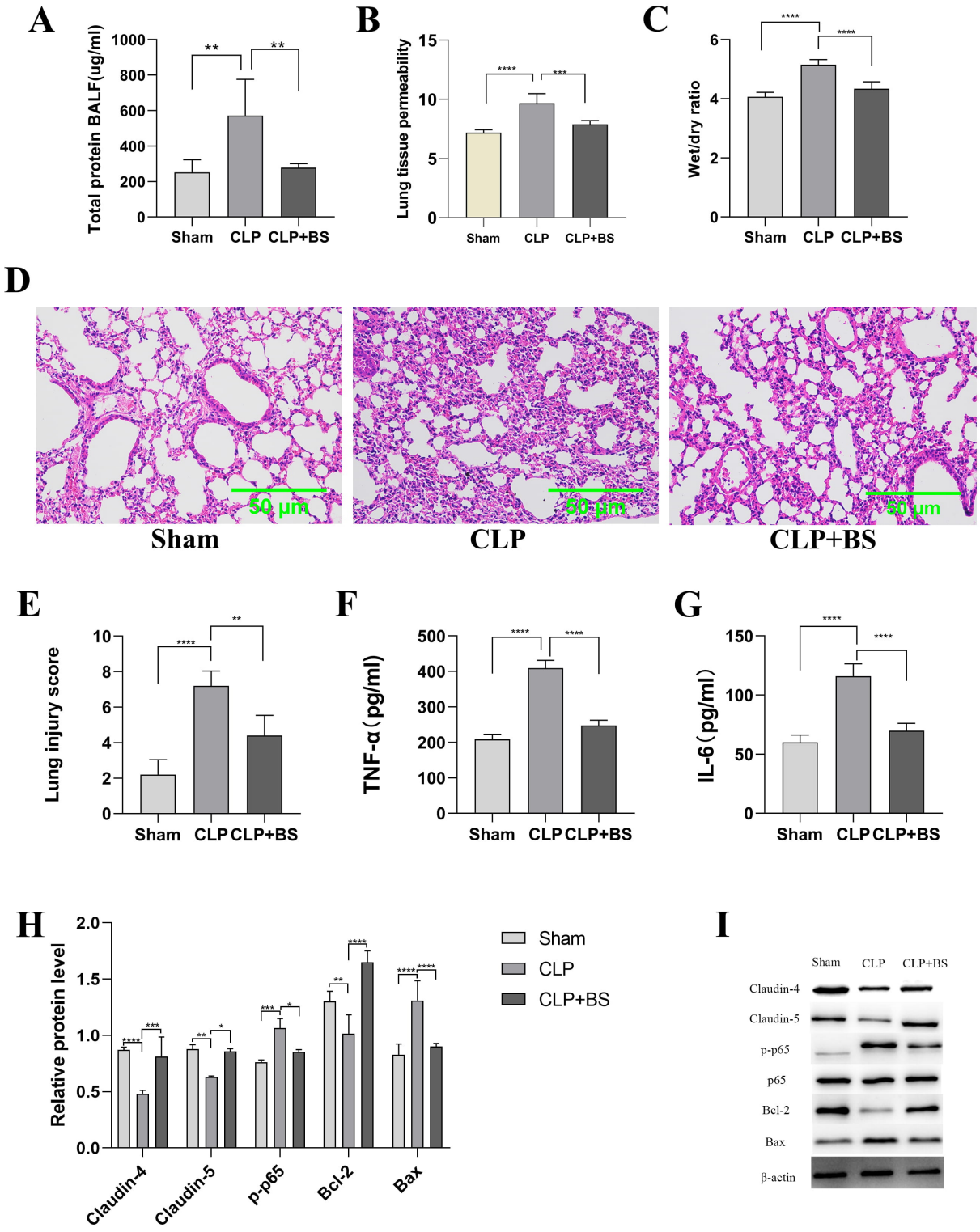

Fig. 1. Effect of beta-sitosterol (BS) on inflammatory response, permeability, and protein expression in septic mice. Bicinchoninic acid (BCA) Protein Concentration Assay Kit assessed the total protein concentration in bronchoalveolar lavage fluid (BALF) (A). Evan's blue staining for determining lung tissue permeability of mice (B). Lung wet/dry ratioof mice from different groups (C). Lung tissues were detected by hematoxylin and eosin (HE) staining to evaluate the severity of lung injury (D). Lung injury scores in each group (E). Enzyme-linked immunosorbent assay (ELISA) for analyzing lung TNF-α (F) and IL-6 (G) levels. Western blotting for detecting the protein levels of claudin-4, claudin-5, p-p65, BAX, and BCL-2 in the lung tissues of mice (H,I). Data were represented as means $\pm$ standard deviation. Significant values are denoted by $^{*}p < 0.05$, $^{**}p < 0.01$, $^{***}p < 0.001$, $^{****}p < 0.0001$, compared to the specified group.

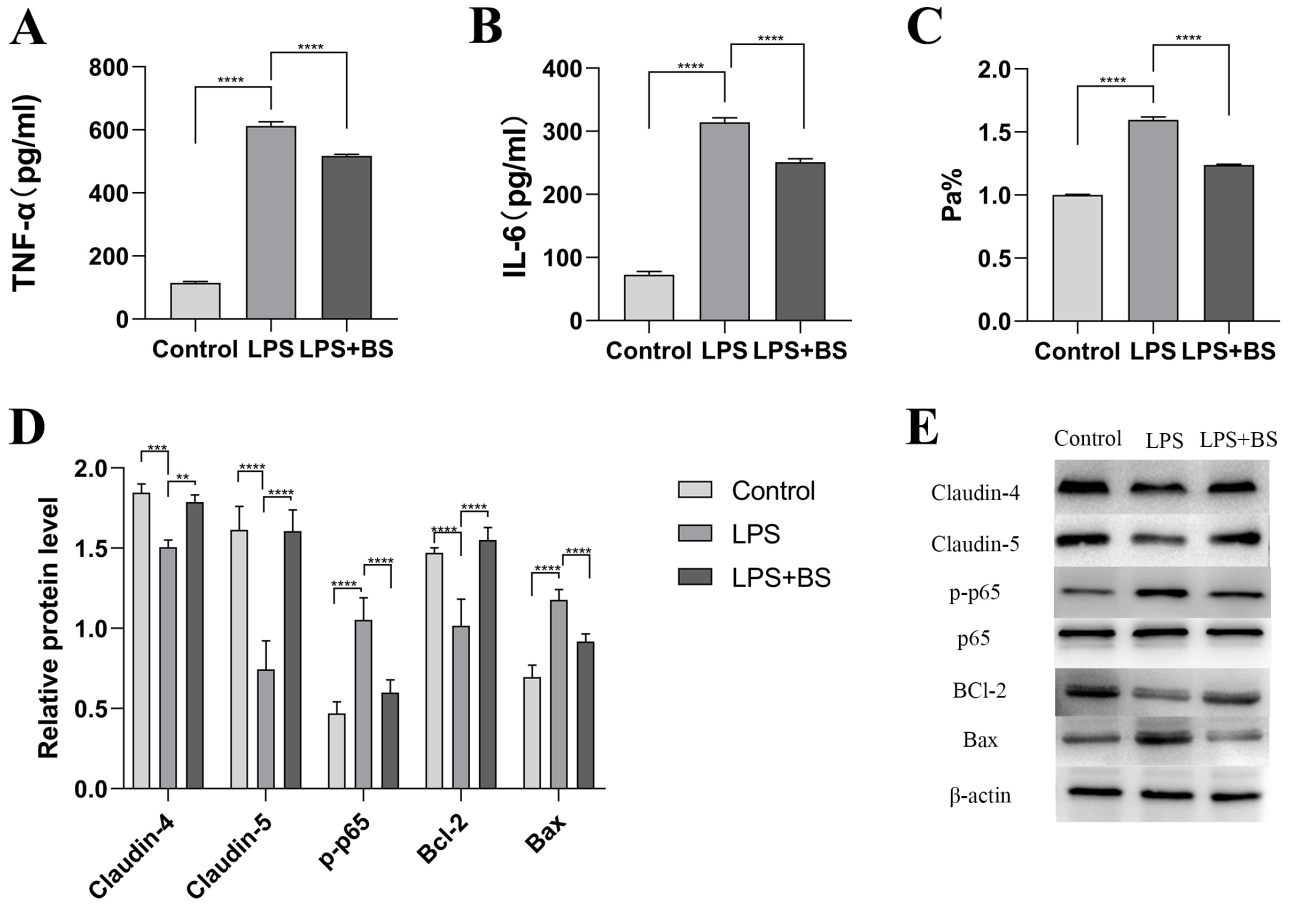

Fig. 2. Effect of BS on inflammatory response, permeability, and protein expression in LPS-stimulated murine lung epithelial (MLE-12) cells. ELISA for detecting TNF-α (A) and IL-6 (B) in the supernatant of MLE-12. Fluorescein isothiocyanate (FITC)-dextran extravasation was used to detect the permeability of the MLE-12 cells monolayer (C). Western blotting for detecting claudin-4, claudin-5, p-p65, BAX and BCL-2 protein levels (D,E). Data were represented as means $\pm$ standard deviation. Significant values are denoted by $^{**}p < 0.01$, $^{***}p < 0.001$, $^{****}p < 0.0001$, compared to the specified group.

Fig. 2C). Nevertheless, treatment with BS ameliorated the increase in MLE-12 cells permeability ($p < 0.0001$), indicating its potential for preserving cell membrane integrity.

BS Mitigates LPS-Induced Permeability Increaseby Increasing Claudin-4 and Claudin-5 Expression

Western blot analysis revealed distinct trends (Fig. 2D,E and Fig. 3D,E). Specifically, after the introduction of LPS stimulation to MLE-12 cells, there was a marked decrease in the expression levels of claudin-5 and claudin-4 ($p < 0.01$), coupled with an observable elevation in the level of p-p65 ($p < 0.01$). However, with the implementation of BS treatment, an opposing outcome was observed: the expression levels of claudin-5 and claudin-4 exhibited a significant increase, while the level of p-p65 demonstrated a significant decrease ($p < 0.001$). A novel approach was undertaken to delve further into the influence of the NF-κB pathway on claudin-5 and claudin-4 protein expression. Cells were exposed to the NF-κB agonist PMA alongside the LPS + BS treatment. This resulted in an increase in the phosphorylation level of p65 ($p < 0.001$), accompanied by a decline in the expression levels of claudin-5 and claudin-4 (Fig. 3D,E). Considering the implications on MLE-12 cell permeability, it was evident that following LPS stimulation, a noticeable escalation in permeability compared to the control group was observed ($p < 0.0001$, Fig. 3C). However, this augmented permeability was effectively mitigated by implementing BS treatment ($p < 0.01$). On the contrary, applying PMA led to a rise in permeability ($p < 0.05$). The outcomes from cellular immunofluorescence experiments mirrored similar trends (Fig. 4).

Discussion

The fundamental strength of the lung's barrier function hinges on the intactness of the pulmonary vascular endothelial and pulmonary epithelial cell barriers. These barriers are intricately upheld by tight junctions, which establish a sturdy framework for air-blood interfaces. Tight

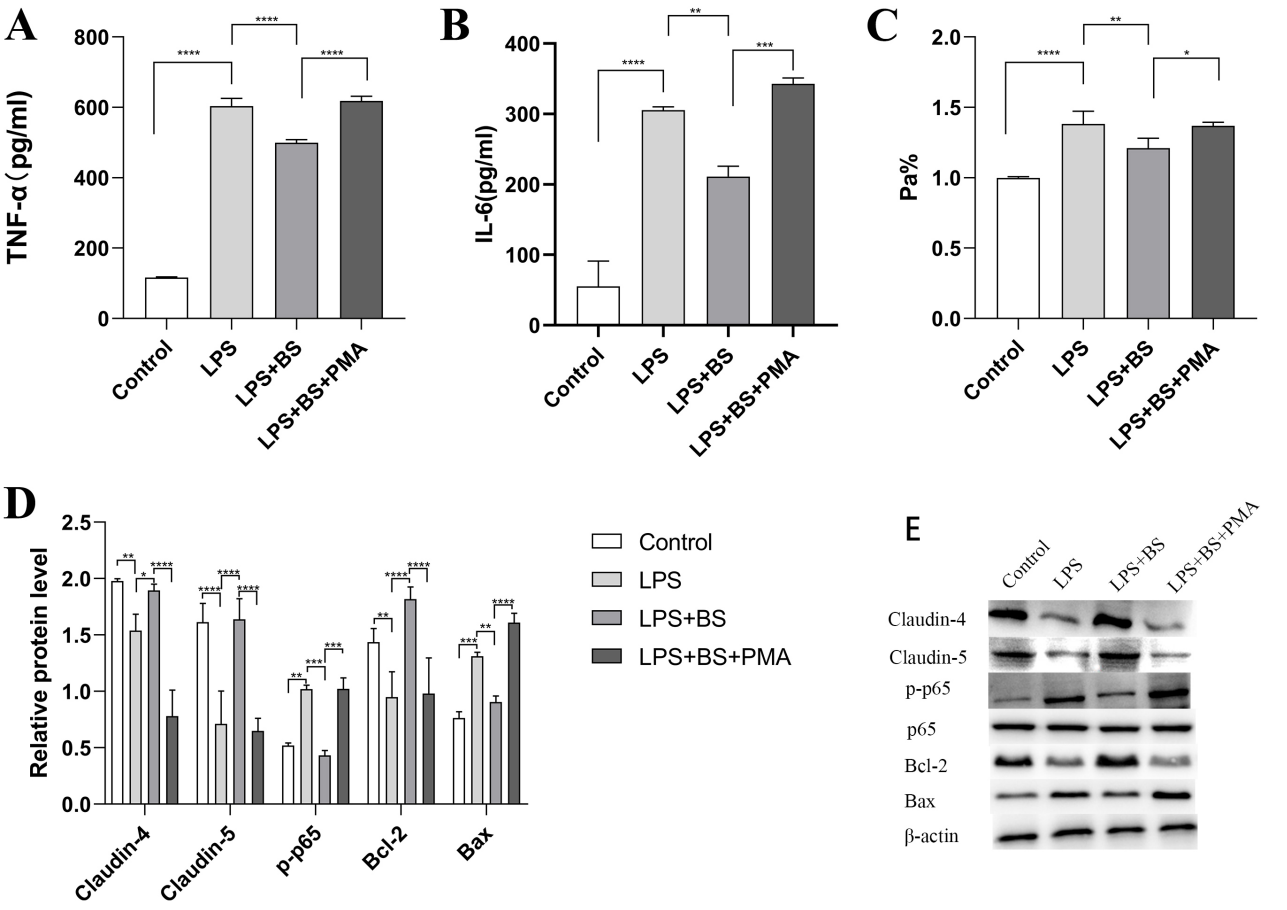

Fig. 3. Effect of BS and phorbol 12-myristate 13-acetate (PMA) on inflammatory response, permeability, and protein expression in LPS-stimulated MLE-12 cells. ELISA for detecting TNF-α (A) and IL-6 (B) in the supernatant of MLE-12. FITC-dextran extravasation was used to detect the permeability of the MLE-12 cells monolayer (C). Western blotting for detecting claudin-4, claudin-5, p-p65, BAX and BCL-2 protein levels in MLE-12 cells (D,E). Data were represented as means $\pm$ standard deviation. Significant values are denoted by $^{*}p < 0.05$, $^{**}p < 0.01$, $^{***}p < 0.001$, $^{****}p < 0.0001$, compared to the specified group.

junctions play a pivotal role in safeguarding this functional interface by averting indiscriminate fluid seepage into the air compartment and thwarting the ingress of inhaled pathogens [20]. During lung inflammation, the foremost factor contributing to the breakdown of the epithelial barrier stems from the impairment endured by tight junctions. The architecture of tight junctions comprises two key categories of proteins: those located within the cell membrane and those associated with the cell membrane periphery. The group of transmembrane proteins within tight junctions encompasses diverse components such as tight junction-associated Marvel proteins, claudins, and members of the immunoglobulin superfamily. In contrast, peripheral membrane proteins linked to tight junctions include F-actin, scaffold proteins that interact with F-actin or do not bind to F-actin, molecules responsible for cell polarity, and factors in cell signaling pathways [21]. Claudin-4 and claudin-5 are examples of claudins, which are critical in maintaining the alveolar epithelial cell barrier function [12,22].

The lung tissue's inflammatory cell infiltration can release significant inflammatory cytokines, including TNF-α and IL-6 [23,24], as in our study when suffering sepsis. These cytokines have the potential to inflict harm upon alveolar epithelial cells, inducing disarray in the structure of the alveoli, heightening the permeability of alveolar epithelial cells, compromising the integrity of the lung barrier, and culminating in the emergence of pulmonary edema [25]. In the HE staining (Fig. 1D), we found that the lung tissue of the CLP sepsis model mice had obvious inflammatory exudation and edema. The involvement of the NF-κB signaling pathway is of paramount importance in the context of acute lung injury (ALI), as it assumes a pivotal role in the initiation of transcription for an array of inflammatory genes [26]. Consequently, this amplifies the severity of lung injury stemming from sepsis [27].

Moreover, the signaling pathway in question holds the capacity to exert control over the expression of tight junction proteins situated within epithelial cells. This regulatory effect, in turn, contributes to the compromise of the epithe-

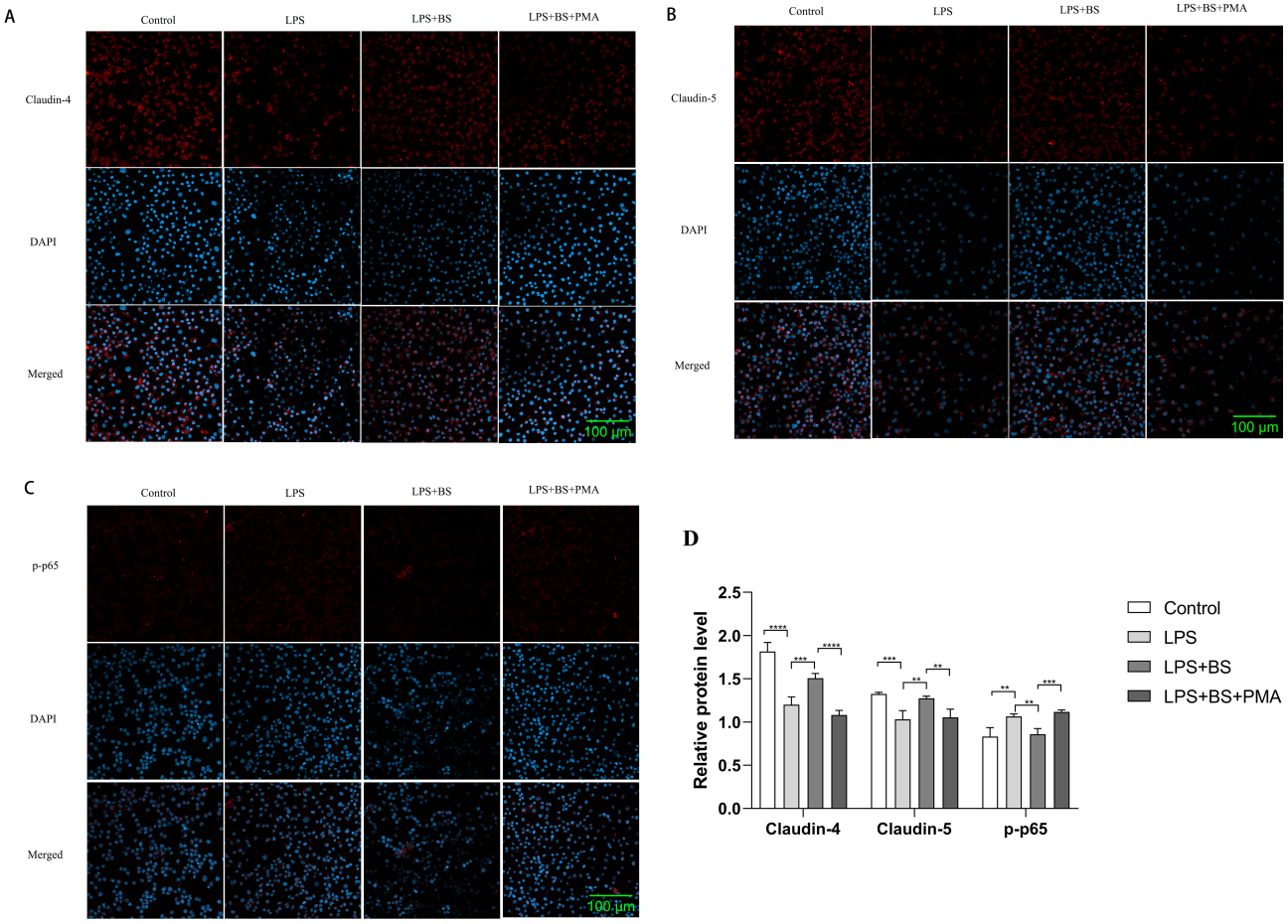

Fig. 4. Cell immunofluorescence. Cell immunofluorescence for detecting the protein levels of Claudin-4 (A), Claudin-5 (B), and p-p65 (C) in MLE-12 cells. The relative protein levels (D). Significant values are denoted by $^{**}p < 0.01$, $^{***}p < 0.001$, $^{****}p < 0.0001$, compared to the specified group.

lial cell barrier function [28]. We also observed similar results: activation of NF-κB signaling impairs lung epithelial barrier function.

Numerous studies have demonstrated the potent anti-inflammatory effects of BS [14,15,29,30]. These effects can be attributed to its ability to inhibit macrophage secretion of inflammatory factors, reduce the expression of NLRP3 (a key component of NLRP3 inflammatory vesicles), and effectively inhibit NF-κB activation. Furthermore, the application of BS has demonstrated its capability to hinder the detrimental immune reaction orchestrated by retinoic acid-inducible gene I (*RIG-I*) and interferon, leading to a reduction in lung injury stemming from infection with the influenza A virus [31]. A separate investigation demonstrated that BS counteracts alveolar epithelial-mesenchymal transition through TGF-β1/Snail pathway inhibition, effectively curbing lung fibrosis [32]. These observations indicate that BS could be a potent guardian of lung health during inflammatory conditions. Our research additionally unveiled BS's competence in diminishing the generation of pro-inflammatory agents like TNF-α and IL-6, dampening the activation of NF-κB p65 in both animal and cellular trials, alongside promoting claudin-4 and claudin-5 expression, thus alleviating the inflammation-driven escalation in alveolar epithelial cell permeability.

BS has demonstrated significant antitumor effects by inducing apoptotic tumor cell death. Research has illuminated the prospective capacity of BS to induce apoptosis within non-small cell lung cancer cells by stimulating p53 activation, fostering the expression of BAX, and orchestrating a downregulation of BCL-2 protein. As a result, this culminates in initiating apoptosis within A549 cells [33]. Within ovarian cancer, BS augments the generation of reactive oxygen species and triggers an influx of calcium via the endoplasmic reticulum-mitochondrial axis. This intricate interplay reshapes signaling pathways within human ovarian cancer cells, triggers proapoptotic signals, and disrupts mitochondrial membrane potential, inhibiting cell proliferation and promoting ovarian cancer cell apoptosis [34]. Notably, BS is widely acknowledged for its safety and non-toxic attributes, and it does not induce apoptosis in normal cells [35].

However, in our study, in both cellular and animal models of sepsis, BS exhibited the capacity to enhance

the expression of the anti-apoptotic marker BCL-2 protein while simultaneously reducing the levels of the apoptotic marker BAX protein. This juxtaposition of effects points towards a potential regulatory influence of BS in sepsis. Moreover, a distinct investigation illustrated that BS yielded an increase in BCL-2 expression and a corresponding decrease in caspase-3 expression within a model simulating myocardial ischemia-reperfusion injury. Consequently, this dual effect translated into a reduction in myocardial infarct size and cell apoptosis, underscoring the role of BS as a cardioprotective agent [36]. These findings suggest that BS exerts anti-apoptotic effects in inflammatory states [37].

Conclusions

Our study demonstrates that BS can potentially alleviate sepsis-induced lung injury by inhibiting the NF-κB signaling pathway, thereby attenuating the inflammatory response. Additionally, BS modulates apoptosis and regulates claudin-4 and claudin-5 to protect alveolar epithelial cell barrier function. These findings suggest that BS may be a promising therapeutic agent for treating sepsis-induced lung injury.

Availability of Data and Materials

All data generated or analyzed during this study are included in this published article.

Author Contributions

SN and ZS designed and conceptualized the entire experimental program, and edited the paper. XC, JC, and YR carried out the experiments, analyzed the data, and drafted the manuscript. MW, ZY, and WZ contributed to performing data curation, formal analysis, validation, visualization, and revise the first draft. QL and CL contributed to the investigation, methodology, resources, software, and revising the first draft. All authors have read the final version and agreed to take responsibility for all aspects of the manuscript.

Ethics Approval and Consent to Participate

The experimental procedure was conducted following the Guidelines for the Care and Use of Laboratory Animals and approved by the Ethics Committee of Jinling Hospital, Nanjing School Clinical Medicine, Southern Medical University (Approval NO. 2022DZGKJDWLS-00160).

Acknowledgment

Not applicable.

Funding

This study was supported by the National Natural Science Foundation of China (82172182, 82102311), Natural Science Foundation of Jiangsu Province (BK20211136), Project of Xuzhou Science and Technology Bureau (No.KC22136), Project of Affiliated Hospital of Xuzhou Medical University (No.XYFY202232) and the Project of Peking Union Medical Union Foundation Emergency Rui Yi (No.2022).

Conflict of Interest

The authors declare no conflict of interest.

References

[1] Evans L, Rhodes A, Alhazzani W, Antonelli M, Coopersmith CM, French C, *et al*. Surviving sepsis campaign: international guidelines for management of sepsis and septic shock 2021. Intensive Care Medicine. 2021; 47: 1181–1247.

[2] Rudd KE, Johnson SC, Agesa KM, Shackelford KA, Tsoi D, Kievlan DR, *et al*. Global, regional, and national sepsis incidence and mortality, 1990-2017: analysis for the Global Burden of Disease Study. Lancet (London, England). 2020; 395: 200–211.

[3] Huang SJ, Ai T, Hu H, Wang J, Wang JL. Immunotherapy for Sepsis Induced by Infections: Clinical Evidence and Potential Targets. Discovery Medicine. 2022; 34: 83–95.

[4] Whitney JE, Feng R, Koterba N, Chen F, Bush J, Graham K, *et al*. Endothelial Biomarkers Are Associated With Indirect Lung Injury in Sepsis-Associated Pediatric Acute Respiratory Distress Syndrome. Critical Care Explorations. 2020; 2: e0295.

[5] Li W, Long L, Yang X, Tong Z, Southwood M, King R, *et al*. Circulating BMP9 Protects the Pulmonary Endothelium during Inflammation-induced Lung Injury in Mice. American Journal of Respiratory and Critical Care Medicine. 2021; 203: 1419–1430.

[6] Xie J, Wang H, Kang Y, Zhou L, Liu Z, Qin B, *et al*. The Epidemiology of Sepsis in Chinese ICUs: A National Cross-Sectional Survey. Critical Care Medicine. 2020; 48: e209–e218.

[7] Schlingmann B, Molina SA, Koval M. Claudins: Gatekeepers of lung epithelial function. Seminars in Cell & Developmental Biology. 2015; 42: 47–57.

[8] Mitchell LA, Overgaard CE, Ward C, Margulies SS, Koval M. Differential effects of claudin-3 and claudin-4 on alveolar epithelial barrier function. American Journal of Physiology. Lung Cellular and Molecular Physiology. 2011; 301: L40–L49.

[9] Rokkam D, Lafemina MJ, Lee JW, Matthay MA, Frank JA. Claudin-4 levels are associated with intact alveolar fluid clearance in human lungs. The American Journal of Pathology. 2011; 179: 1081–1087.

[10] Frank JA. Claudins and alveolar epithelial barrier function in the lung. Annals of the New York Academy of Sciences. 2012; 1257: 175–183.

[11] Kage H, Flodby P, Gao D, Kim YH, Marconett CN, DeMaio L, *et al*. Claudin 4 knockout mice: normal physiological phenotype with increased susceptibility to lung injury. American Journal of Physiology. Lung Cellular and Molecular Physiology. 2014; 307: L524–L536.

[12] Kakogiannos N, Ferrari L, Giampietro C, Scalise AA, Maderna C, Ravà M, *et al*. JAM-A Acts via C/EBP-α to Promote Claudin-5 Expression and Enhance Endothelial Barrier Function. Circu-

lation Research. 2020; 127: 1056–1073.

[13] Paniagua-Pérez R, Flores-Mondragón G, Reyes-Legorreta C, Herrera-López B, Cervantes-Hernández I, Madrigal-Santillán O, *et al*. EVALUATION OF THE ANTI-INFLAMMATORY CAPACITY OF BETA-SITOSTEROL IN RODENT ASSAYS. African Journal of Traditional, Complementary, and Alternative Medicines: AJTCAM. 2016; 14: 123–130.

[14] Liao PC, Lai MH, Hsu KP, Kuo YH, Chen J, Tsai MC, *et al*. Identification of β-Sitosterol as in Vitro Anti-Inflammatory Constituent in Moringa oleifera. Journal of Agricultural and Food Chemistry. 2018; 66: 10748–10759.

[15] Kasirzadeh S, Ghahremani MH, Setayesh N, Jeivad F, Shadboorestan A, Taheri A, *et al*. β-Sitosterol Alters the Inflammatory Response in CLP Rat Model of Sepsis by Modulation of NFκB Signaling. BioMed Research International. 2021; 2021: 5535562.

[16] M T, T A, B S, Ak G, Sks S. Curcumin prophylaxis refurbishes alveolar epithelial barrier integrity and alveolar fluid clearance under hypoxia. Respiratory Physiology & Neurobiology. 2020; 274: 103336.

[17] Gu LM, Li H, Xia JQ, Pan CY, Gu C, Tian YZ. Huangqin Decoction Attenuates DSS-Induced Mucosal Damage and Promotes Epithelial Repair via Inhibiting TNF-α-Induced NF-κB Activation. Chinese Journal of Integrative Medicine. 2022; 28: 124–129.

[18] Yang CH, Tsai PS, Wang TY, Huang CJ. Dexmedetomidine-ketamine combination mitigates acute lung injury in haemorrhagic shock rats. Resuscitation. 2009; 80: 1204–1210.

[19] Wang L, Wu J, Guo X, Huang X, Huang Q. RAGE Plays a Role in LPS-Induced NF-κB Activation and Endothelial Hyperpermeability. Sensors (Basel, Switzerland). 2017; 17: 722.

[20] Tobioka H, Tokunaga Y, Isomura H, Kokai Y, Yamaguchi J, Sawada N. Expression of occludin, a tight-junction-associated protein, in human lung carcinomas. Virchows Archiv: an International Journal of Pathology. 2004; 445: 472–476.

[21] Godbole NM, Chowdhury AA, Chataut N, Awasthi S. Tight Junctions, the Epithelial Barrier, and Toll-like Receptor-4 During Lung Injury. Inflammation. 2022; 45: 2142–2162.

[22] Yang J, Wang Y, Liu H, Bi J, Lu Y. C2-ceramide influences alveolar epithelial barrier function by downregulating Zo-1, occludin and claudin-4 expression. Toxicology Mechanisms and Methods. 2017; 27: 293–297.

[23] Ehrentraut H, Weisheit CK, Frede S, Hilbert T. Inducing Acute Lung Injury in Mice by Direct Intratracheal Lipopolysaccharide Instillation. Journal of Visualized Experiments. 2019; 1–7.

[24] Matute-Bello G, Frevert CW, Martin TR. Animal models of acute lung injury. American Journal of Physiology. Lung Cellular and Molecular Physiology. 2008; 295: L379–L399.

[25] Abdelmoneim M, El-Naenaeey ESY, Abd-Allah SH, Gharib AA, Alhussein M, Aboalella DA, *et al*. Anti-Inflammatory and Immunomodulatory Role of Bone Marrow-Derived MSCs in Mice with Acute Lung Injury. Journal of Interferon & Cytokine Research: the Official Journal of the International Society for Interferon and Cytokine Research. 2021; 41: 29–36.

[26] Liu TY, Zhao LL, Chen SB, Hou BC, Huang J, Hong X, *et al*. *Polygonatum sibiricum* polysaccharides prevent LPS-induced acute lung injury by inhibiting inflammation via the TLR4/Myd88/NF-κB pathway. Experimental and Therapeutic Medicine. 2020; 20: 3733–3739.

[27] Yang H, Lv H, Li H, Ci X, Peng L. Oridonin protects LPS-induced acute lung injury by modulating Nrf2-mediated oxidative stress and Nrf2-independent NLRP3 and NF-κB pathways. Cell Communication and Signaling: CCS. 2019; 17: 62.

[28] Lin JC, Wu JQ, Wang F, Tang FY, Sun J, Xu B, *et al*. QingBai decoction regulates intestinal permeability of dextran sulphate sodium-induced colitis through the modulation of notch and NF-κB signalling. Cell Proliferation. 2019; 52: e12547.

[29] Jayaraman S, Devarajan N, Rajagopal P, Babu S, Ganesan SK, Veeraraghavan VP, *et al*. β-Sitosterol Circumvents Obesity Induced Inflammation and Insulin Resistance by down-Regulating IKKβ/NF-κB and JNK Signaling Pathway in Adipocytes of Type 2 Diabetic Rats. Molecules (Basel, Switzerland). 2021; 26: 2101.

[30] Loizou S, Lekakis I, Chrousos GP, Moutsatsou P. Beta-sitosterol exhibits anti-inflammatory activity in human aortic endothelial cells. Molecular Nutrition & Food Research. 2010; 54: 551–558.

[31] Zhou BX, Li J, Liang XL, Pan XP, Hao YB, Xie PF, *et al*. β-sitosterol ameliorates influenza A virus-induced proinflammatory response and acute lung injury in mice by disrupting the cross-talk between RIG-I and IFN/STAT signaling. Acta Pharmacologica Sinica. 2020; 41: 1178–1196.

[32] Park YJ, Bang IJ, Jeong MH, Kim HR, Lee DE, Kwak JH, *et al*. Effects of β-Sitosterol from Corn Silk on TGF-β1-Induced Epithelial-Mesenchymal Transition in Lung Alveolar Epithelial Cells. Journal of Agricultural and Food Chemistry. 2019; 67: 9789–9795.

[33] Rajavel T, Packiyaraj P, Suryanarayanan V, Singh SK, Ruckmani K, Pandima Devi K. β-Sitosterol targets Trx/Trx1 reductase to induce apoptosis in A549 cells via ROS mediated mitochondrial dysregulation and p53 activation. Scientific Reports. 2018; 8: 2071.

[34] Bae H, Park S, Ham J, Song J, Hong T, Choi JH, *et al*. ER-Mitochondria Calcium Flux by β-Sitosterol Promotes Cell Death in Ovarian Cancer. Antioxidants (Basel, Switzerland). 2021; 10: 1583.

[35] Paniagua-Pérez R, Madrigal-Bujaidar E, Reyes-Cadena S, Molina-Jasso D, Gallaga JP, Silva-Miranda A, *et al*. Genotoxic and cytotoxic studies of beta-sitosterol and pteropodine in mouse. Journal of Biomedicine & Biotechnology. 2005; 2005: 242–247.

[36] Lin F, Xu L, Huang M, Deng B, Zhang W, Zeng Z, *et al*. β-Sitosterol Protects against Myocardial Ischemia/Reperfusion Injury via Targeting PPARγ/NF-κB Signalling. Evidence-based Complementary and Alternative Medicine: ECAM. 2020; 2020: 2679409.

[37] Mahmoud MS, El-Kott AF, AlGwaiz HIM, Fathy SM. Protective effect of Moringa oleifera Lam. leaf extract against oxidative stress, inflammation, depression, and apoptosis in a mouse model of hepatic encephalopathy. Environmental Science and Pollution Research International. 2022; 29: 83783–83796.